



Communication

Improving the Performance of Bidirectional Communication System Using Second-Order Raman Amplifiers

Zhongshuai Feng , Peili He, Wei Li ^{*}, Kaijing Hu , Fei Tong and Xingrui Su

Wuhan National Laboratory for Optoelectronic, Huazhong University of Science and Technology, Wuhan 430074, China; zsfeng@hust.edu.cn (Z.F.); m202173338@hust.edu.cn (P.H.); d202281179@hust.edu.cn (K.H.); m202273374@hust.edu.cn (F.T.); M202473490@hust.edu.cn (X.S.)

* Correspondence: weilee@hust.edu.cn

Abstract: In order to achieve low-cost scalability, the same-wavelength bidirectional (SWB) fiber communication system is a better solution. We present a detailed investigation of the performance of the different orders Raman amplifiers in same-wavelength bidirectional fiber communication systems. We discuss how to suppress the main factor affecting system performance which is Rayleigh scattering noise (RSN). By using different Raman amplifiers to construct different quasi-lossless transmission, the performance changes in the same-wavelength bidirectional fiber optic communication system were studied. On this basis, multi-channel and same-wavelength single fiber bidirectional system experiments were conducted to compare the performance of second-order Raman systems and first-order Raman systems. The results indicate that the Rayleigh scattering suppression effect of second-order Raman systems is better, and compared to first-order Raman systems, the average signal-to-noise ratio (SNR) can be increased by 2.88 dB.

Keywords: bidirectional system; backscattering noise; distributed Raman amplifier; quasi-lossless transmission



Citation: Feng, Z.; He, P.; Li, W.; Hu, K.; Tong, F.; Su, X. Improving the Performance of Bidirectional Communication System Using Second-Order Raman Amplifiers.

Photonics **2024**, *11*, 879. <https://doi.org/10.3390/photonics11090879>

Received: 26 August 2024

Revised: 17 September 2024

Accepted: 17 September 2024

Published: 19 September 2024



Copyright: © 2024 by the authors. Licensee MDPI, Basel, Switzerland. This article is an open access article distributed under the terms and conditions of the Creative Commons Attribution (CC BY) license (<https://creativecommons.org/licenses/by/4.0/>).

1. Introduction

In recent years, with the vigorous development of high-tech such as virtual reality, video conferencing, and 5G, global data traffic has shown an explosive growth trend, which is continuously putting pressure on the capacity of current fiber optic communication systems [1–3]. New fiber optic communication expansion solutions are urgently needed. In fact, there is currently a technology similar to wireless duplex that is gradually being applied in fiber optic communication systems [4–8], which is the same-wavelength bidirectional coherent optical communication system studied in this article. This technology has great prospects in expanding the capacity of existing fiber optic systems. It can increase the system capacity without changing the current link conditions. Ideally, it can double the transmission capacity of existing fiber optic communication systems; it is possible to exceed the limit of 100 Tbit/s for the transmission capacity of ordinary single-mode optical fibers. It has many advantages such as low cost, high symmetry, easy implementation, management, and maintenance. However, unlike wireless communication systems, fiber optic communication systems are difficult to operate in the same-wavelength single fiber bidirectional mode due to the reflection interference along the fiber, especially the inherent Rayleigh scattering noise [9,10]. Therefore, studying and even suppressing crosstalk in these systems is of great significance. At the same time, for applications such as time-frequency synchronization and PON [11], their inherent application scenarios are single fiber bidirectional scenarios, which naturally face interference from the above factors.

Therefore, it is important to explore how to suppress adverse factors in single fiber bidirectional systems. In this regard, many scholars have explored it. In 2019, Yasser Chiniforoshan et al. investigated the transmission capacity benefits of bidirectional coherent optical communication with the same wavelength compared to traditional single

fiber unidirectional transmission systems. The results showed that this scheme can bring an additional 50% to 100% capacity improvement [12]. In 2021, Wenbo Yu and his team demonstrated a real-time transmission experiment with a capacity of 16 Tbit/s in the C-band based on the same-wavelength bidirectional coherent optical communication system. They studied the effects of Fresnel reflection, Rayleigh scattering, and Amplified Spontaneous Emission Noise (ASE) on the performance of single fiber bidirectional systems, and the results showed that the system has the best tolerance for Fresnel reflection, while the tolerance for Rayleigh scattering crosstalk is equivalent to ASE noise. In addition, it was found in the experiment that the nonlinear crosstalk introduced by the opposite signal in the bidirectional transmission system has a very small impact [13]. In 2021, You Wang et al. proposed a digital signal processing (DSP) method based on Linear Frequency Modulated Training Sequence (LFMTS) to effectively suppress Fresnel reflection in bidirectional coherent optical communication systems with the same wavelength [14]. In 2023, the team proposed that lossless transmission has the best effect on suppressing the signal-to-noise ratio. Experimental verification was conducted using a first-order Raman system, which showed an improvement in the signal-to-noise ratio compared to erbium-doped fiber amplifier (EDFAs)-based systems [15]. But the team only verified the quasi-lossless system constructed by the first-order Raman system, and the degree of losslessness of the constructed system is not enough. In 2024, Muyang Mei et al. conducted preliminary research on the influence of SRS in first-order Raman systems. In order to explore the better degree of non-destructive testing and the impact of introducing high-order Raman on single fiber bidirectional systems, we analyzed different order Raman systems and compared the performance differences in single fiber bidirectional systems under different order Raman systems through experiments.

2. Principle

Rayleigh scattering noise is formed by the accumulation of a large amount of Rayleigh backscattered light, with a high degree of randomness, ultimately resulting in scattering crosstalk being indistinguishable from signal light in common dimensions such as amplitude, polarization, phase, and frequency, making it difficult to further suppress it directly. However, the transmission path of the signal is unidirectional, while RSN is formed by the accumulation of countless Rayleigh scattered light, whose paths are looped in the fiber, as shown in Figure 1a. Due to the different paths between the signal and RSN, the output power also varies. By changing the distribution gain and loss in the fiber, the deviation in output power may be amplified. In fact, fiber loss is difficult to change, but distributed gain can be adjusted through distributed Raman amplifiers. This reveals that distributed Raman amplifier (DRA) can be configured to minimize the signal to RSN power ratio (SRR), which means that RSN has been effectively suppressed.

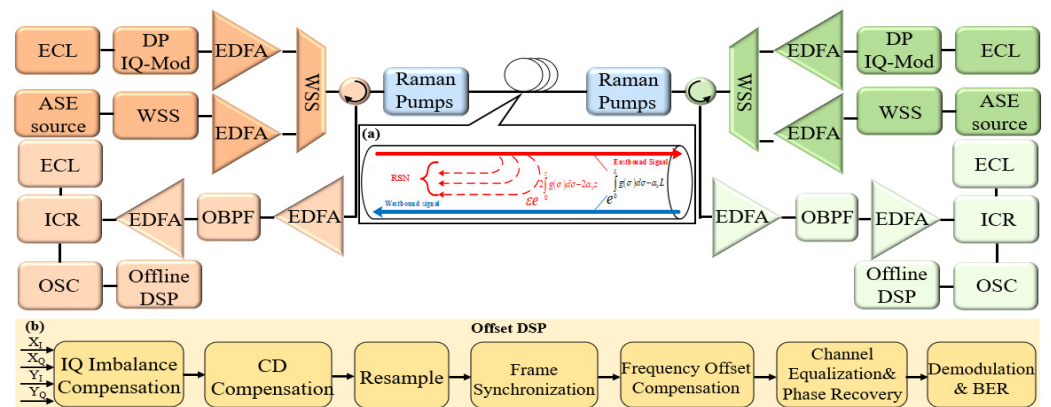


Figure 1. The experimental setup diagram of the SWB scheme based on DRAs; (a) schematic of the transmission and accumulation of the signal and RSN in fibers; the red and blue thick arrows are signal, the red dashed arrow is RSN; (b) the structure of receiver DSP.

At the receiving end, the power of signal light and Rayleigh scattering crosstalk light considering the influence of distributed gain can be expressed as follows:

$$P_{sig}(L) = P_0 \exp\left(\int_0^L g(\sigma)d\sigma - a_s L\right), \tag{1}$$

$$P_{RSN}(L) = \varepsilon P_0 \int_0^L \exp\left(\int_0^z 2g(\sigma)d\sigma - 2a_s z\right) dz, \tag{2}$$

where L is the fiber length, P_0 is the emission power of signal light, $g(\sigma)$ is the distributed gain coefficient, a_s is the fiber loss, and ε is the Rayleigh backscatter coefficient.

According to the definition of SRR, it can be represented in the following form:

$$\frac{1}{SRR} = \frac{P_{RSN}(L)}{P_{sig}(L)} = \varepsilon \int_0^{\frac{L}{2}} \left\{ \frac{f(z)}{f\left(\frac{L}{2}\right)} \exp(-2\alpha_s z) + \frac{f\left(\frac{L}{2}\right)}{f\left(\frac{L}{2} - z\right)} \exp\left[-2\alpha_s\left(z + \frac{L}{2}\right)\right] \right\} dz. \tag{3}$$

It can be seen that when $g(\sigma) = \alpha_s$, SRR can take the maximum value. DRA is very helpful for this, but in order to achieve better quasi lossless effects, higher-order Raman pumping is required. However, correspondingly, higher-order Raman amplifiers also introduce greater noise. It is necessary to compare the performance of different order Raman amplifiers in single fiber bidirectional systems. In this article, we have demonstrated through experiments that high-order DRAs have a better inhibitory effect on RSN.

3. Experimental Setup

The experimental schematic is shown in Figure 1. Two bidirectional transmitters were designed to generate 120 channels in the super C-band, with an interval of 50 GHz and a wavelength range of 1524 nm to 1572 nm. Fourteen channels were monitored, while the remaining channels were simulated by filtering ASE noise. The channel under test (CUT) is generated by modulating a tunable laser (linewidth < 100 kHz) with a dual polarization in-phase orthogonal modulator, which is driven by a 92 GSa/s arbitrary waveform generator and configured to provide 48 Gbaud DP-64 QAM.

The spectrum of CUT is compressed by a rising cosine filter with a roll off coefficient of 0.1. The booster EDFA before fiber optic connection is designed to provide a maximum output power of 18.5 dBm. The optical link between two circulators was composed of 80 km G.652 fibers and DRA. The experiment used six Raman pumps with wavelengths of 1340 nm, 1360 nm, 1425 nm, 1435 nm, 1455 nm, and 1465 nm to suppress RSN. The first-order Raman only uses the first-order pumps, which are 1425 nm, 1435 nm, 1455 nm, and 1465 nm. The second-order Raman use both the second-order pumps, which are 1340 nm, 1360 nm, and the first-order pumps, which are 1425 nm, 1435 nm, 1455 nm, 1465 nm. The first-order pumps of the second-order Raman is used as seed pump. In order to achieve the best pump power configuration within the 80 km range of G.652 fiber, bit error ratio (BER) and SNR scans were performed on 4 representative CUTs, during which the power of the second-order pumps and the first-order pumps was set to be equal, separately. Additionally, the first-order pumps of the second-order Raman is fixed as 50 mW. The results using only first-order DRA and second-order DRA are shown in Figure 2a,b, respectively. The results indicate that when using first-order DRAs, the first-order pumps power should all be set to 200 mW, and when using second-order DRAs, the first-order pumps power should all be set to 50 mW and the second-order pumps power should all be set to 500 mW to achieve the best suppression of RSN. Because in this configuration, both SNR and BER are optimal values. We noticed that for low frequencies, BER/SNR with second-order DRA seems less sensitive to pump power than first-order DRA. This is mainly due to the size of the pump

power. The direct reason for the significant changes in the results of first-order DRA is that its pump power starts from 0. When the pump power starts from 100, its BER/SNR changes slowly. Meanwhile, when the pump power of the first-order DRA is low, inter channel stimulation becomes more pronounced. Therefore, it will lead to this result.

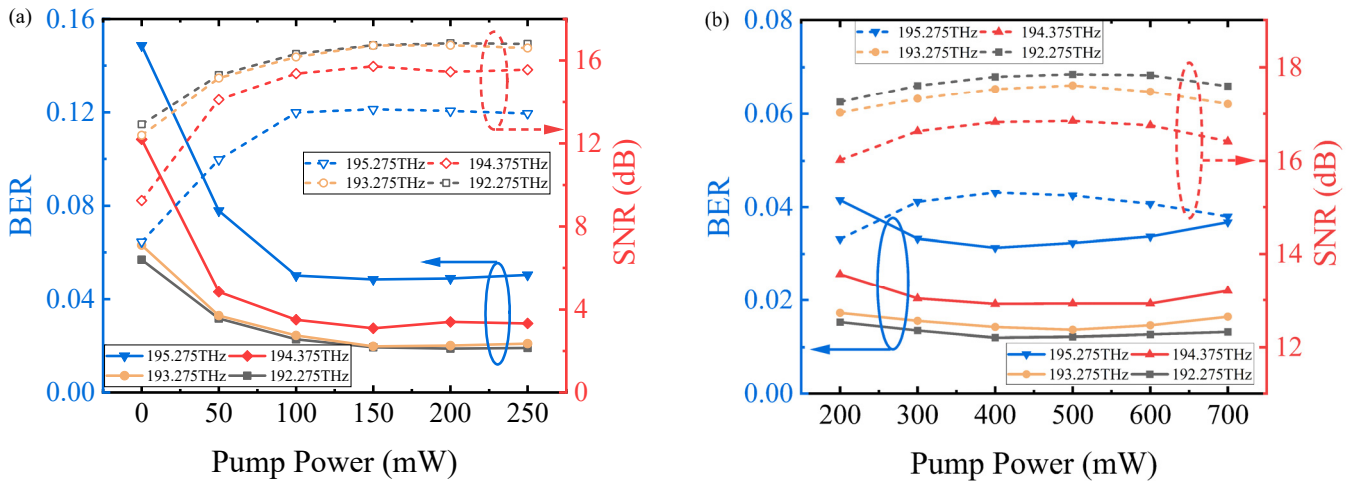


Figure 2. The measured SNR and BER as functions of pump’s power of (a) 1st-order DRAs and (b) 2nd-order DRAs. The bold lines correspond to BER results and the dashed lines correspond to SNR.

At the receiving end, the EDFA after fiber optic connection is designed to amplify the received signal. An optical bandpass filter (OBPF) is used to suppress the amplified spontaneous emission (ASE) noise. Due to the high insertion loss of OBPF, the EDFA after OBPF is designed to amplify the received signal. Subsequently, the signal is detected by an Integrated Coherent Receiver (ICR), which is connected to an oscilloscope with a 3 dB bandwidth of 36 GHz and a sampling rate of 80 GSa/s. In the DSP of the receiver, the phase orthogonal imbalance compensation algorithm is first used to process the electrical signal. After performing dispersion compensation and resampling operations, the frame synchronization algorithm is implemented using a specially designed pilot sequence. Then, the signal is processed using the frequency offset compensation algorithm, and combined with the phase recovery algorithm, the multi-input–multi-output equalizer is processed. Finally, the bit error rate and signal-to-noise ratio of the received signal are obtained through demodulation, demapping, and decoding.

4. Transmission Results and Discussion

The experimental results are shown in Figure 3. Figure 3a records the measured signal-to-noise ratios of 14 CUTs for unidirectional and bidirectional transmission on G.652 fibers at 80 km using first-order DRA. Figure 3b records the measured signal-to-noise ratios of 14 CUTs for unidirectional and bidirectional transmission on G.652 fibers at 80 km using dual-order DRA. They are all measured under the optimal power configuration. For both first-order and second-order Raman systems, first transmit bidirectional signals simultaneously and measure the SNR of the signal at the receiving end. Then, turn off the signal in one direction, keep the other parts of the link unchanged, and measure the SNR of the signal at the receiving end. This can ensure that the main impact on the system is Rayleigh scattering noise. For both first-order and second-order Raman systems, their performance in bidirectional systems decreases compared to unidirectional systems, where SNR has all decreased. What is important is the signal contamination by the Raman-amplified Rayleigh scattering from the signal traveling in the opposite direction. But the performance of second-order Raman systems decreases less, which means they are less affected by Rayleigh scattering interference. Obviously, second-order DRA effectively suppresses RSN, resulting in a signal-to-noise ratio loss of only about 0.4 dB

using second-order DRA and 1.1 dB using first-order DRA. This is because, as we analyzed in Section 2, during transmission, the signal undergoes a complete fiber and undergoes a complete Raman gain process. However, some of the Rayleigh scattering only undergoes a partial fiber, so it can only be subjected to a partial Raman gain process. Therefore, distributed gain will have different effects on signal and Rayleigh scattering. Different gains can also lead to different effects. Comparing the measured signal-to-noise ratios of 14 CUTs using first-order DRA and second-order DRA under bidirectional transmission conditions, as shown in Figure 4, the results show that the signal-to-noise ratios have both improved, with an average signal-to-noise ratio increase of 2.88 dB. Because when facing the same Rayleigh scattering, the distributed gain provided by second-order DRA is more conducive to suppressing Rayleigh scattering. This indicates that applying second-order Raman to single fiber bidirectional systems is highly effective and can effectively improve system performance.

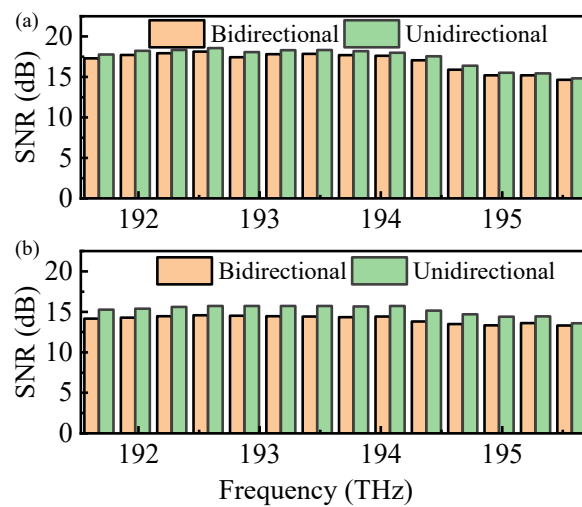


Figure 3. (a,b) are the measured SNR of 14 CUTs under unidirectional and bidirectional transmission over G.652 fibers with length of 80 km by using 2nd-order DRAs and 1st-order DRAs, respectively.

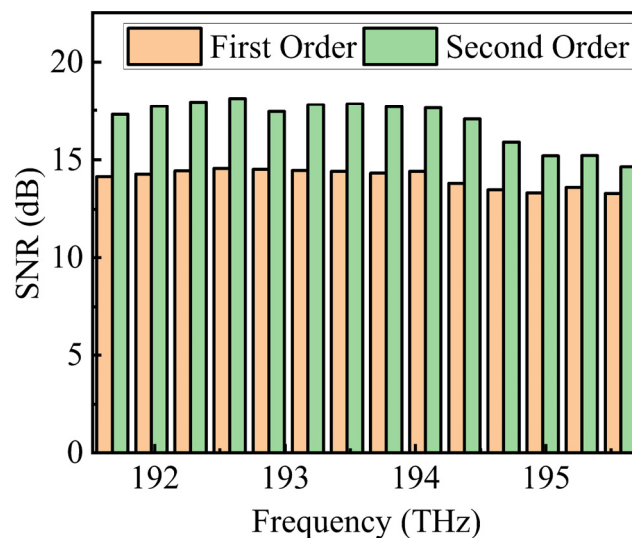


Figure 4. The measured SNR of 14 CUTs under bidirectional transmission by using 1st-order DRAs and 2nd-order DRAs.

Figure 5 shows the BER of 14 CUTs. Due to the influence of RSN, the signal quality of SWB scheme is significantly reduced compared to unidirectional systems. However, the BER of each channel is still almost below the threshold required by 25% FEC. Based on the

FEC overhead required for each channel, the actual communication capacity of each channel can be calculated. For bidirectional systems, if 25% FEC is uniformly used for each channel, the actual capacity of each channel is 0.92 Tbit/s, and the total communication capacity is 110.6 Tbit/s. Please note that the quality of the high-frequency channel has deteriorated, which may be due to the Raman transfer effect. Due to the Raman transfer effect, the energy in the high-frequency part is transferred to the low-frequency part. Therefore, the distributed gain experienced by the high-frequency part has decreased, making it unable to effectively suppress Rayleigh scattering, resulting in a gradual decline in its performance. This is more evident on second-order DRA. Due to the decrease in Raman gain, the performance of second-order DRA in the high-frequency range will approach that of first-order DRA. This means that the configuration of the Raman pump needs further optimization. For example, adding high-frequency pumps, but due to the experimental conditions, it is difficult to carry out this part of the work.

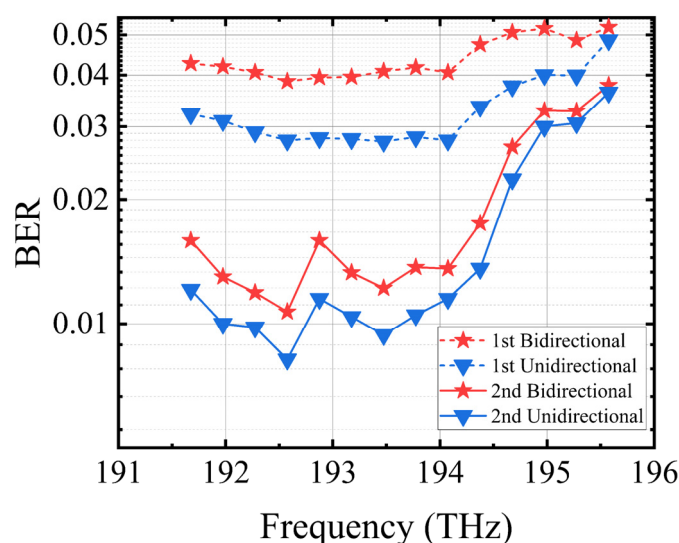


Figure 5. BER as a function of operation frequency for the 14 evaluated CUTs.

5. Conclusions

In this article, we demonstrate that second-order DRA is more effective in suppressing RSN in SWB systems. Firstly, we have derived that Rayleigh scattering noise is better suppressed under lossless transmission conditions in theory. Then, we validate it by constructing different quasi-lossless transmission systems using different Raman amplifiers. The experimental research is conducted on the ultra c-band DWDM SWB fiber transmission system with a load of 120×48 Gbaud DP-64 QAM on an 80 km G.652 fiber. The results show that, in SWB systems, second-order DRA can provide better RSN suppression effect, and the transmission effect is better than first-order DRA. This will provide a new approach to improving the performance of SWB systems.

Author Contributions: Conceptualization, Z.F. and W.L.; methodology, Z.F.; software, Z.F.; validation, Z.F. and P.H.; formal analysis, Z.F.; investigation, Z.F.; resources, W.L.; data curation, Z.F.; writing—original draft preparation, Z.F.; writing—review and editing, K.H., F.T. and X.S.; visualization, Z.F.; supervision, W.L.; project administration, K.H., F.T. and X.S.; funding acquisition, W.L. All authors have read and agreed to the published version of the manuscript.

Funding: This research received no external funding.

Institutional Review Board Statement: Not applicable.

Informed Consent Statement: Not applicable.

Data Availability Statement: The data presented in this study are available on request from the corresponding author.

Conflicts of Interest: The authors declare no conflicts of interest.

References

1. Yuan, H.; Furdek, M.; Muhammad, A.; Saljoghei, A.; Wosinska, L.; Zervas, G. Space-division multiplexing in data center networks: On multi-core fiber solutions and crosstalk-suppressed resource allocation. *J. Opt. Commun. Netw.* **2018**, *10*, 272–288. [[CrossRef](#)]
2. Rademacher, G.; Puttnam, B.J.; Luís, R.S.; Eriksson, T.A.; Fontaine, N.K.; Mazur, M.; Chen, H.; Ryf, R.; Neilson, D.T.; Sillard, P. Peta-bit-per-second optical communications system using a standard cladding diameter 15-mode fiber. *Nat. Commun.* **2021**, *12*, 4238. [[CrossRef](#)] [[PubMed](#)]
3. Rademacher, G.; Puttnam, B.J.; Luís, R.S.; Sakaguchi, J.; Klaus, W.; Eriksson, T.A.; Awaji, Y.; Hayashi, T.; Nagashima, T.; Nakanishi, T.; et al. 10.66 Peta-Bit/s Transmission over a 38-Core-Three-Mode Fiber. In Proceedings of the Optical Fiber Communication Conference (OFC) 2020, OSA Technical Digest (Optica Publishing Group, 2020), San Diego, CA, USA, 8–12 March 2020; paper Th3H.1.
4. Qian, D.; Huang, M.-F.; Zhang, S.; Zhang, Y.; Huang, Y.-K.; Yaman, F.; Djordjevic, I.B.; Mateo, E. 30 Tb/s C- and L-bands bidirectional transmission over 10,181 km with 121 km span length. *Opt. Express* **2013**, *21*, 14244–14250. [[CrossRef](#)] [[PubMed](#)]
5. Pintus, P.; Andriolli, N.; Di Pasquale, F.; Bowers, J.E. Bidirectional Crosstalk and Back-Reflection Free WDM Active Optical Interconnects. *IEEE Photonics Technol. Lett.* **2013**, *25*, 1973–1976. [[CrossRef](#)]
6. Li, Q.; Hu, L.; Zhang, J.; Chen, J.; Wu, G. Fiber Radio Frequency Transfer Using Bidirectional Frequency Division Multiplexing Dissemination. *IEEE Photonics Technol. Lett.* **2021**, *33*, 660–663. [[CrossRef](#)]
7. Nga, N.T.; Sangirov, J.; Joo, G.C.; Yoo, B.S.; Ukaegbu, I.A.; Lee, T.W.; Cho, M.H.; Park, H.H. 10 Gbps/ch Full-Duplex Optical Link Using a Single-Fiber Channel for Signal Transmission. *IEEE Photonics Technol. Lett.* **2014**, *26*, 609–612. [[CrossRef](#)]
8. Rapp, L.; Azendorf, F.; Eiselt, M. Performance Impact of Signal Reflections in a Single-Fiber Bidirectional System. *IEEE Photonics Technol. Lett.* **2021**, *33*, 1411–1414. [[CrossRef](#)]
9. Ko, J.; Kim, S.; Lee, J.; Won, S.; Kim, Y.S.; Jeong, J. Estimation of performance degradation of bidirectional WDM transmission systems due to Rayleigh backscattering and ASE noises using numerical and analytical models. *J. Light. Technol.* **2003**, *21*, 938–946.
10. Deventer, M. Fundamentals of bidirectional transmission over a single optical fiber. *Solid-State Sci. Technol. Libr.* **1994**, *2*, 993–996.
11. Feng, Q.; Li, W.; Zheng, Q.; Han, J.; Xiao, J.; He, Z.; Luo, M.; Yang, Q.; Yu, S. Impacts of backscattering noises on upstream signals in full-duplex bidirectional PONs. *Opt. Express* **2015**, *23*, 15575–15586. [[CrossRef](#)] [[PubMed](#)]
12. Chiniforooshan, Y.; Tang, X.; Jiang, Z.; Zhang, Z. High Capacity Coherent Systems Using Same-Wavelength Bidirectional Transmission. In Proceedings of the 2019 Asia Communications and Photonics Conference (ACPC), Chengdu, China, 2–5 November 2019.
13. Yu, W.; Shi, H.; Liu, Y.; Shang, W.; Jia, Y.; Feng, Z. Experimental demonstration of 160x100 Gb/s real-time WDM bidi-transmission over 100-km G.652 fiber. In Proceedings of the 2021 Asia Communications and Photonics Conference (ACP), Shanghai, China, 24–27 October 2021.
14. Wang, Y.; Li, W. LFMTS-assisted reflection interference elimination method for a coherent same-wavelength bidirectional optical communication system. *Opt. Express* **2021**, *29*, 20077–20091. [[CrossRef](#)] [[PubMed](#)]
15. Wu, C. Same-Wavelength Bidirectional Coherent Fiber Communication Scheme with OSNR Improved by Raman Amplifiers. *J. Light. Technol.* **2023**, *41*, 7336–7345. [[CrossRef](#)]

Disclaimer/Publisher’s Note: The statements, opinions and data contained in all publications are solely those of the individual author(s) and contributor(s) and not of MDPI and/or the editor(s). MDPI and/or the editor(s) disclaim responsibility for any injury to people or property resulting from any ideas, methods, instructions or products referred to in the content.